The ROI CT problem: a shearlet-based regularization approach

Journal of Physics: Conference Series **756** (2016) 012009 doi:10.1088/1742-6596/756/1/012009

The ROI CT problem: a shearlet-based regularization approach

T A Bubba[1], F Porta[2], G Zanghirati[2] and S Bonettini[2]

[1] Dipartimento di Scienze Fisiche, Informatiche e Matematiche, Università di Modena e Reggio Emilia, Via Campi 213/b, 41125 Modena, Italy

[2] Dipartimento di Matematica e Informatica, Università di Ferrara, Via Saragat 1, 44122 Ferrara, Italy

E-mail: tatiana.bubba@unimore.it, federica.porta@unife.it, g.zanghirati@unife.it, silvia.bonettini@unife.it

Abstract. The possibility to significantly reduce the X-ray radiation dose and shorten the scanning time is particularly appealing, especially for the medical imaging community. Region-of-interest Computed Tomography (ROI CT) has this potential and, for this reason, is currently receiving increasing attention. Due to the truncation of projection images, ROI CT is a rather challenging problem. Indeed, the ROI reconstruction problem is severely ill-posed in general and naive local reconstruction algorithms tend to be very unstable. To obtain a stable and reliable reconstruction, under suitable noise circumstances, we formulate the ROI CT problem as a convex optimization problem with a regularization term based on shearlets, and possibly nonsmooth. For the solution, we propose and analyze an iterative approach based on the variable metric inexact line-search algorithm (VMILA). The reconstruction performance of VMILA is compared against different regularization conditions, in the case of fan-beam CT simulated data. The numerical tests show that our approach is insensitive to the location of the ROI and remains very stable also when the ROI size is rather small.

1. Introduction

Region-of-interest Computed Tomography (ROI CT) is an X-ray based incomplete data imaging acquisition modality [1]. Since X-ray radiation exposure comes with health hazards for patients, the possibility to reconstruct only a small ROI using truncated projection data is particularly appealing, especially in biomedical application, due to its potential to lower the X-ray radiation dose and reduce the scanning time. However, reconstructing a density function from its projections is an ill-posed problem, with the ill-posedness becoming more severe when projections are truncated, as in the case of ROI CT. Therefore, traditional approaches, like Filtered Back-Projection, in general produce unacceptable visual artifacts and are unstable to noise.

To address the problem of ROI reconstruction from truncated projections, a variety of *ad hoc* methods, both analytic and algebraic, were proposed in the last years (see [2] and the references therein), but usually require restrictive hypothesis on the ROI or are rather sensitive to noise.

To overcome these drawbacks, we formulate ROI CT as a convex optimization problem with a regularized objective function, possibly nonsmooth, and based on a very recently introduced multiscale method called shearlets [3]. The use of less recent multiscale methods is not new in CT application, even combined with analytic approaches [4]. The approach we present

partially relies on the setup in [5]. However, our approach differs in the objective function, which considers shearlets instead of wavelets, and in the aim, since our goal is to compare the different regularization terms proposed to identify the model which better provides the desired features of the image to reconstruct. Moreover, for the solution of the minimization problems we exploit a very recently proposed algorithm belonging to the class of proximal-gradient techniques, the variable metric inexact line-search algorithm (VMILA) [6], in place of a (split) augmented Lagrangian. VMILA is a proximal-gradient method, which enables the inexact computation of the proximal point defining the descent direction and guarantees the sufficient decrease of the objective function by means of an Armijo–like backtracking procedure. In order to evaluate the effectiveness of the suggested theoretical approaches we conduct a numerical study on simulated data. In particular, we investigate which approach produces the most accurate ROI reconstruction, without any assumption on the ROI size or location.

2. Region-of-interest tomography setup

In the ROI tomography problem, measurements are taken only within a limited region-of-interest (generally, a disk) strictly inside the object support. The goal is to reconstruct the density function inside the ROI only from these truncated data.

This can be accomplished by using the mask function $M(\theta,\tau) = 1_{\mathcal{P}(S)}(\theta,\tau)$ which selects the set $\mathcal{P}(S) = \{(\theta,\tau) \in \mathcal{T} : \ell(\theta,\tau) \cap S \neq \emptyset\}$ of those rays meeting the ROI, where 1_A is the characteristic function of the set A, S the ROI disk, $\ell(\theta,\tau) = \{\mathbf{x} \in \mathbb{R}^2 : \langle \mathbf{x}, \omega_\theta \rangle = \tau\}$ denotes a ray, being $\omega_\theta = (\cos(\theta), \sin(\theta))^T$, and $\mathcal{T} = \{(\theta,\tau) : \theta \in [0, 2\pi), \tau \in \mathbb{R}\}$ the tangent space. Namely, the *truncated sinogram* $y_0(\theta,\tau)$ shall be given by:

$$y_0(\theta,\tau) = M(\theta,\tau)\, \mathcal{R}f(\theta,\tau), \tag{1}$$

where $\mathcal{R}f(\theta,\tau) = \int_{\ell(\theta,\tau)} f(\mathbf{x})\, d\mathbf{x}$ is the Radon transform of the density function $f \in \mathbb{R}^2$ [7]. In the following, we will address as *full sinogram* the Radon projections

$$y(\theta,\tau) = \mathcal{R}f(\theta,\tau). \tag{2}$$

In particular, equation (2) can be used as a global constraint to fix an extrapolation scheme which defines y outside $\mathcal{P}(S)$. Indeed, the following equation

$$y = y_0 + (1 - M)y. \tag{3}$$

suggests to interpret ROI CT as an extrapolation problem, where, given y_0 on $\mathcal{P}(S)$, the goal is to extrapolate this function to the region outside $\mathcal{P}(S)$. Clearly, not *any* extrapolation scheme is suitable to define y outside $\mathcal{P}(S)$ and equation (2) ensures that y is the image of the Radon transform of the same density function $f \in L^1(\mathbb{R}) \cap L^2(\mathbb{R})$. From (2), we derive two conditions:

$$M\mathcal{R}f = M\, y = y_0 \qquad \text{(data fidelity)} \tag{4}$$

$$(1 - M)\mathcal{R}f = (1 - M)\, y \qquad \text{(data consistency)} \tag{5}$$

Notice that the data fidelity equation defines a constraint inside the ROI while the data consistency equation enforces accurate reconstruction inside the ROI.

Equations (4) and (5) alone do not lead to a unique solution. Indeed, the least square solution

$$\hat{f} = \arg\min_f \|M\mathcal{R}f - y_0\|_2^2,$$

is not unique, since, in general, the solution of the ROI CT problem is not guaranteed to be unique [7]. When uniqueness is ensured, the ill-posedness is too severe, due to the truncation

of projections. A classical approach to achieve uniqueness is to impose an additional norm condition, according to Tikhonov regularization, and this norm condition can be applied in the image domain or in the (Radon) transform domain. Hence, we define a norm condition in the transform domain by posing:

$$\|f\|_2^2 = \frac{1}{4\pi}\left\|I^{-\frac{1}{2}}\mathcal{R}f\right\|_2^2$$

given that $f=(4\pi)^{-1}\mathcal{R}^*I^{-1}\mathcal{R}f$ holds true [7, p. 11], where $\mathcal{R}^*$ is the adjoint of the operator $\mathcal{R}$ (usually referred to as backprojection operator), and $I^{-1/2}$ is the Riesz potential operator [7, p. 5]. Thus, we are lead to the following optimization problem:

$$\hat{f} = \underset{f}{\operatorname{argmin}}\, \Upsilon_2(f) \qquad \text{s. t.} \quad y = \mathcal{R}f \quad \text{and} \quad My = y_0 \tag{6}$$

with $\Upsilon_2(f) = \|I^{-1/2}\mathcal{R}f\|_2^2$. By analogy, we can modify the optimization problem using the functional $\Upsilon_p(f) = \|I^{-1/2}\mathcal{R}f\|_p^p$ with $1 \leq p \leq 2$. In the following, we will use $p = 1$, that can be interpreted as a sparsity-promoting condition. The discrete counterpart of (6) reads as:

$$\hat{\mathbf{f}} = \underset{\mathbf{f}}{\operatorname{argmin}}\, \|\mathbf{\Phi W f}\|_p^p \qquad \text{s. t.} \quad \mathbf{y} = \mathbf{W f} \quad \text{and} \quad \mathbf{M y} = \mathbf{y}_0 \tag{7}$$

where $\mathbf{W}$ is the forward projection matrix, representing the map from the image domain to the projection domain. It is sized $N_\theta N_{\text{dtc}} \times N^2$, with N_θ number of projection angles, N_{dtc} number of detector cells and N is both the width and the height in pixels of the object to reconstruct. The elements of the matrix $\mathbf{W}$ are computed according to the distance-driven method [8]. The diagonal matrix $\mathbf{M}$, sized $N_\theta N_{\text{dtc}} \times N_\theta N_{\text{dtc}}$, is the mask corresponding to the ROI, whose entries are either 0 or 1. The unknown discrete density function $\mathbf{f}$ is a vector of length N^2, while the full and truncated sinogram $\mathbf{y}$ and $\mathbf{y}_0$ are vectors of length $N_\theta N_{\text{dtc}}$, all obtained by column-wise stacking the entries of the corresponding matrices. Finally, $\mathbf{\Phi}$ is a discrete filter *corresponding* to the Riesz potential operator $I^{-1/2}$. Indeed, in place of considering a straightforward matrix discretization of the Riesz potential operator, we approximate it by using a discrete shearlet transform [3], whose corresponding matrix is denoted by $\mathbf{\Phi}$. The underlying idea is to exploit the shearlets optimally sparse approximation properties, which are particularly relevant in CT-like applications, since point-like structures in the image domain map onto sine-shaped curvilinear structures in the projection domain [9]. Formulation (7) is equivalent to the following formulation:

$$\begin{gathered}\hat{\mathbf{f}} = \underset{\mathbf{f}\in\mathbb{R}^{N^2}}{\operatorname{argmin}}\, \mathbf{\Psi}(\mathbf{f}) \qquad \text{where} \\ \mathbf{\Psi}(\mathbf{f}) = \frac{1}{2}\|\mathbf{MWf} - \mathbf{y}_0\|_2^2 + \lambda\, \|\mathbf{\Phi}((\mathbf{I}_{N_\theta N_{\text{dtc}}} - \mathbf{M})\mathbf{Wf} + \mathbf{y}_0)\|_p^p + \iota_{\Omega_\mathbf{f}}.\end{gathered} \tag{8}$$

In (8) we considered the L^2-norm error of the data fidelity equation and we incorporated the data consistency information in the regularization term. Here, λ denotes the regularization parameter and $\iota_{\Omega_\mathbf{f}}$ is the indicator function of the feasible region which is defined as $\mathbf{f} \geq 0$ or $0 \leq \mathbf{f} \leq L$, where L is the image maximum pixel intensity and the inequalities are meant component-wise. Notice that each term of the objective function is convex with respect to the unknown. In the following, we compare two different models belonging to (8) and obtained by selecting $p = 2$ or $p = 1$.

3. Numerical Experiments

To demonstrate and validate our approach, we use the synthetic data set known as "modified Shepp-Logan phantom" sized $N \times N$ pixels with $N = 128$, which is available, for instance, in

Table 1. Optimal results for shearlet-based regularization (8) with $p = 1$, 2, and $\lambda = 10^{-4}$.

	$\sigma = 0.05$									$\sigma = 0.1$								
	$\mathbf{r}_{\text{ROI}} = 0.25N$			$\mathbf{r}_{\text{ROI}} = 0.15N$			$\mathbf{r}_{\text{ROI}} = 0.1N$			$\mathbf{r}_{\text{ROI}} = 0.25N$			$\mathbf{r}_{\text{ROI}} = 0.15N$			$\mathbf{r}_{\text{ROI}} = 0.1N$		
	iter	value	sec	iter	value	sec	iter	value	sec	iter	value	sec	iter	value	sec	iter	value	sec
	ROI PSNR									ROI PSNR								
Sm	83	35.86	4.7	109	33.61	6.0	106	32.57	5.8	77	35.49	5.3	111	35.37	7.6	102	37.12	6.9
NSm	83	36.94	15.1	78	41.98	14.2	48	45.43	8.6	48	37.76	10.5	72	40.92	15.9	62	44.64	13.6
	ROI Relative error									ROI Relative error								
Sm	83	0.21	4.7	109	0.57	6.0	106	1.06	5.8	77	0.23	5.3	111	0.46	7.6	102	0.63	6.9
NSm	83	0.19	15.1	78	0.22	14.2	48	0.24	8.6	48	0.17	10.5	72	0.25	15.9	62	0.26	13.6

the Matlab Image Processing toolbox. All the algorithms are implemented in Matlab 8.1.0 and the experiments performed on a dual CPU server, equipped with two 6-cores Intel Xeon X5690 at 3.46GHz, 188 GB DDR3 central RAM memory and up to 12 TB of disk storage.

All the numerical experiments are carried out in the framework of 2D fan-beam geometry. A full angle scan (182 views over 2π) with complete data was simulated. The matrix $\mathbf{\Phi}$ is generated by using the *classical shearlet* decomposition. In details, the number of scales for the shearlet transform is set equal to 4 and the number of directions across the scales is set to (8, 8, 16, 16).

Truncated projection data are obtained by discarding the samples outside the ROI projection $\mathcal{P}(S)$. In particular, we consider concentric ROI disks with decreasing radius $\mathbf{r}_{\text{ROI}}$, placed off-center with respect to the field of view. The results in this paper cover ROIs which are fully inside the object being imaged, according to the hypothesis of the interior tomography problem. Here, we assume that the noise which corrupts the projection data is described by a white Gaussian process, with zero mean and variance σ.

To evaluate the goodness of model (8) by varying the regularization term, we investigated two different formulations: a smooth one with $p = 2$ and a nonsmooth one with $p = 1$. The solution of both the corresponding optimization problems has been addressed by using VMILA. It is a proximal-gradient (or forward-backward) method suitable for minimizing the sum of a differentiable, possibly nonconvex, function plus a convex, possibly nondifferentiable, function. Both the considered formulations for the ROI CT problem are suitable to be faced by such an algorithm. Indeed, in the smooth framework, the differentiable part consists of the first two terms of (8) and the nondifferentiable contribute reduces to the indicator function of the feasible set $\Omega_{\mathbf{f}}$. In the nonsmooth setting, the differentiable term is given by the L^2-norm of the data fidelity and the nondifferentiable one takes into account both $\iota_{\Omega_{\mathbf{f}}}$ and the data consistency regularizer. The VMILA $(k+1)$-th iteration for the minimization of the sum of a smooth function Γ_0 and a nonsmooth one Γ_1 is given by:

$$\mathbf{f}^{(k+1)} = \mathbf{f}^{(k)} + \lambda_k \left\{ \text{prox}^{D_k^{-1}}_{\alpha_k \Gamma_1} \left(\mathbf{f}^{(k)} - \alpha_k D_k \nabla \Gamma_0(\mathbf{f}^{(k)}) \right) - \mathbf{f}^{(k)} \right\}$$

where λ_k is a linesearch parameter, α_k is a positive steplength, D_k is a symmetric and positive definite scaling matrix and $\text{prox}^{D_k^{-1}}_{\alpha_k \Gamma_1}$ denotes the proximal operator associated to Γ_1. VMILA global convergence is ensured by a generalized Armijo-like backtracking procedure to select λ_k. Moreover, $\alpha_k \in [\alpha_{\min}, \alpha_{\max}] \subset \mathbb{R}^+$ and $D_k \in D_\mu$, where $D_\mu = \{D = \text{diag}(d_1, \ldots, d_N) \,|\, d_j \in [\mu^{-1}, \mu] \; \forall j\}$ with $\mu > 1$. For both formulations, we select α_k through an adaptive strategy based on the Barzilai-Borwein updating rules [10, 11] and D_k according to a split-gradient idea [12] based on the decomposition of the gradient of Γ_0 into a positive and a negative part.

In many common situations, including ROI CT, a closed-form of the proximal operator of Γ_1 is not known. In this case, VMILA consists in a double loop method, where the inner loop,

Figure 1. Optimal reconstructions of the Shepp-Logan phantom for decreasing radii and $\sigma = 0.05$. First row: smooth formulation. Second row: nonsmooth formulation.

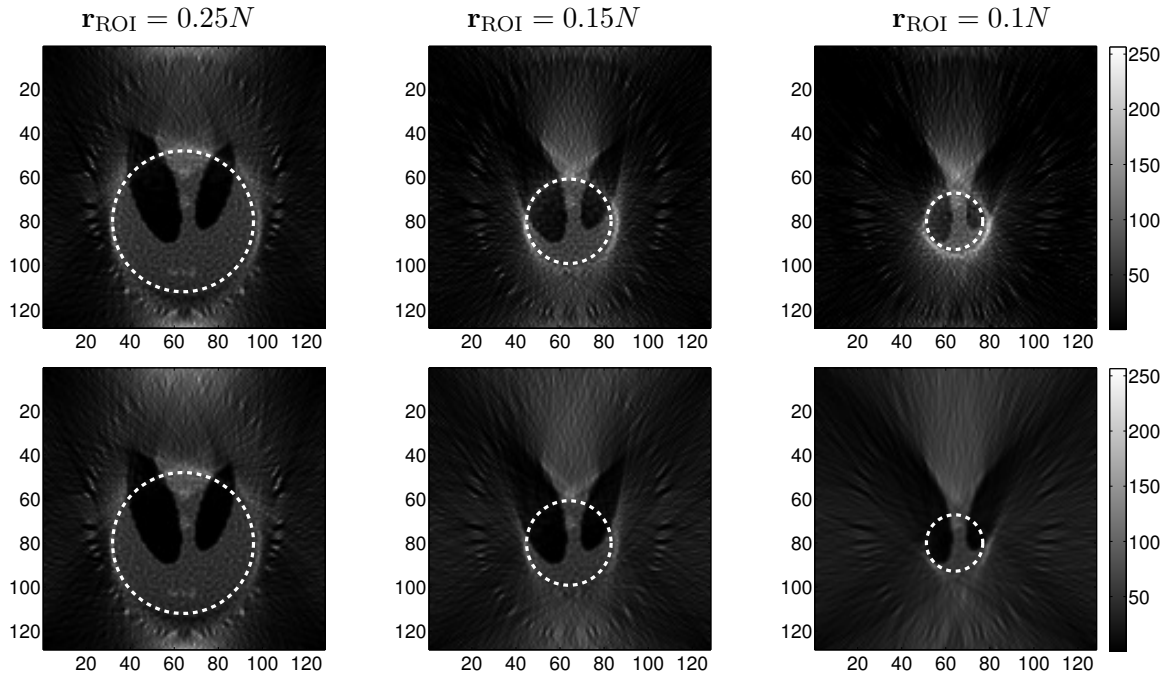

designed to inexactly solve the minimization problem associated to the definition of the proximal operator, is devised with a suitable stopping criterion. For the ROI CT problem, if $p = 1$ we need to compute an approximation of the proximal point which defines the VMILA direction; on the other hand, if $p = 2$, the proximal operator corresponding to the nondifferentiable term of the objective function reduces to the scaled euclidean projection onto the feasible set and therefore no inner loop is required.

We investigated the performance of both the models for regularization parameters $\lambda = 10^{\ell}$, with $\ell = -4, -3, \ldots, 4$. As figures of merit, we use the peak-signal-to-noise ratio (PSNR) and the relative error. We stress that both PSNR and relative error are evaluated inside the ROI only, since ROI CT aims to recover the image only inside the ROI.

Due to room constraint, we summarize in Table 1 only the best results, with respect to the figures of merit, obtained with the shearlet-based formulation for both smooth (Sm) and nonsmooth (NSm) cases, and for two levels of noise, namely $\sigma = 0.05$ (Table 1, left-hand side) and $\sigma = 0.1$ (Table 1, right-hand side). The corresponding images, only for the case $\sigma = 0.05$, are reported in Figure 1. We stress that many additional tests were performed for both formulations, with different level of noise, and also exploiting other regularization approaches, such as smooth total variation (sTV) and early stopping. For instance, for all ROI radii in Table 1 the sTV approach with $\rho = 1$ and $\sigma = 0.05$ yields PSNR = 37.81, 42.93, 47.25, relative error equal to 0.17, 0.19, 0.20, and iter = 107, 145, 172 in 7.3, 9.7, 11.7 seconds, respectively, while with $\sigma = 0.1$, it yields PSNR = 39.21, 44.94, 49.69, relative error equal to 0.14, 0.15, 0.15, and iter = 114, 137, 181 in 7.6, 9.4, 12.3 seconds, respectively. Worse performances were obtained for $\rho = 10^{-2}, 10^{-1}, 10$. These results are *slightly* better than the (nonsmooth) shearlets-based approach, but this is clearly dependent on the phantom features (which is piecewise constant) and may not hold for more general data. We expect that, using more realistic sinograms, the contribution of the shearlet term will become more relevant for the regularization. Evidence of this can be found in [9].

The results in Table 1 show that the nonsmooth formulation outperforms the smooth approach, and this is even more evident as the radius $\mathbf{r}_{\mathrm{ROI}}$ gets smaller. Indeed, when $\sigma = 0.05$, the smooth reconstruction exhibits a 100% ROI relative error for $\mathbf{r}_{\mathrm{ROI}} = 0.1N$, while the nonsmooth reconstruction achieves 24%. This is definitively confirmed by the corresponding images, where no artifacts are visible for the nonsmooth reconstructions, while the smooth ones suffer from low contrast between the smallest features and mild checkerboard effect. Notice that, concerning the figures of merit, the difference between the two approaches is less remarkable when $\sigma = 0.1$, while for the corresponding images (not reported here) similar considerations hold true. However, all the reconstructions are sufficiently good, on a visual basis, since all the fundamental features are detected, and the transition between the ROI to the non-ROI is smooth enough.

For baseline comparison, the analytic approach called Filtered Back-Projection (FBP) with $\sigma = 0.05$ yields PSNR = 27.88, 27.58, 28.49, and rel. err. = 0.54, 1.14, 1.69, respectively. These results are considerably worse than the ones obtained with VMILA. Similar results are obtained with $\sigma = 0.1$. The corresponding images are blurred, suffer from cupping artifacts and the details are not sharp. Some other results, for the smooth case, can be found in [13, 14].

4. Conclusions

In this paper, we presented a numerical assessment on the solution of the ROI CT problem via an iterative minimization method. Two different types of objective functions, namely smooth and nonsmooth, have been considered, aiming at making the reconstruction from truncated data stable. The experiments show that the reconstructions obtained by considering the nonsmooth approach are the best ones, with respect to the figures of merit. A possible explanation might be that the use of the 1-norm leads to the suppression of many small shearlet coefficients in favor of few large shearlet coefficients, that are associated to edges. This allows to separate the structural components of the image from the noise, and this roughly corresponds to denoising. Overall, the reported results show that accurate ROI reconstructions can be obtained regardless of the location and size of the ROI and for rather small ROI sizes using both formulations of the objective function.

Acknowledgments

This work is supported by INdAM-GNCS, the Italian national research project FIRB2012, grant n. RBFR12M3AC, FAR2014-UniFE and FAR2014-UniMORE.

References

[1] Quinto E T 2006 *Proc. of Symposia in Appl. Math.* **63** 1–23
[2] Clackdoyle R and Defrise M 2010 *IEEE Signal Processing* **60** 60–80
[3] Kutyniok G and Labate D 2012 *Shearlets. Multiscale Analysis for Multivariate Data* (Boston, MA (USA): Birkhäuser)
[4] Bonnet S, Peyrin F, Turjman F and Prost R 2002 *IEEE Trans. Image Processing* **11**(3) 169–76
[5] Goossens B, Labate D and Bodmann B 2016 *Private communication*
[6] Bonettini S, Loris I, Porta F and Prato M 2016 *SIAM J. Optim.* **26**(2) 891–921
[7] Natterer F and Wübbeling F 2001 *Mathematical methods in image reconstruction* (Philadelphia, PA (USA): SIAM)
[8] De Man B and Basu S 2004 *Physics in Medicine and Biology* **7** 2463–75
[9] Vandeghinste B, Goossens B, Van Holen R, Vanhove C *et al.* 2013 *IEEE Trans. Nuclear Science* **5** 3305–17
[10] Barzilai J and Borwein J M 1988 *IMA J. Numer. Anal.* **8** 141–8
[11] Frassoldati G, Zanghirati G and Zanni L 2008 *J. Industrial and Management Optim.* **4**(2) 299–312
[12] Lantéri H, Roche M, Cuevas O and Aime C 2001 *Signal Process.* **81** 945–74
[13] Bubba T A, Labate D, Zanghirati G, Bonettini S and Goossens B 2015 *SPIE Optics & Photonics, Wavelets And Applications XVI* vol 9597 (San Diego, CA, USA) p 95970K
[14] Bubba T A, Labate D, Zanghirati G and Bonettini S 2015 *ArXiv e-prints* (*Preprint* `1511.04336`)